

Impact of the Aging Lens and Posterior Capsular Opacification on Quantitative Autofluorescence Imaging in Age-Related Macular Degeneration

Andreas Berlin^{1,2}, Mark E. Clark¹, Thomas A. Swain¹, Nathan A. Fischer¹, Gerald McGwin, Jr^{1,3}, Kenneth R. Sloan¹, Cynthia Owsley¹, and Christine A. Curcio¹

¹ Department of Ophthalmology and Visual Sciences, School of Medicine, University of Alabama at Birmingham, Birmingham, AL, USA

² University Hospital Würzburg, Würzburg, Germany

³ Department of Epidemiology, School of Public Health, University of Alabama at Birmingham, Birmingham, AL, USA

Correspondence: Christine A. Curcio, Department of Ophthalmology and Visual Sciences, EyeSight, Foundation of Alabama Vision Research Laboratories, 1670 University Boulevard Room 360, University of Alabama at Birmingham, School of Medicine, Birmingham, AL 35294-0099, USA. e-mail: christinecurcio@uabmc.edu

Received: March 3, 2022

Accepted: September 20, 2022

Published: October 14, 2022

Keywords: age-related macular degeneration (AMD); quantitative fundus autofluorescence (qAF); cataract; pseudophakia; posterior capsule opacification (PCO); retinal pigment epithelium (RPE)

Citation: Berlin A, Clark ME, Swain TA, Fischer NA, McGwin G Jr, Sloan KR, Owsley C, Curcio CA. Impact of the aging lens and posterior capsular opacification on quantitative autofluorescence imaging in age-related macular degeneration. *Transl Vis Sci Technol.* 2022;11(10):23. <https://doi.org/10.1167/tvst.11.10.23>

Purpose: The purpose of this study was to investigate quantitative autofluorescence (qAF8) in patients with and without early or intermediate age-related macular degeneration (AMD); to determine the impact of the aged crystalline lens and posterior capsular opacification (PCO).

Methods: In phakic and pseudophakic eyes ≥ 60 years, AMD status was determined by the Beckman system. PCO presence and severity was extracted from clinical records. qAF8 was calculated using custom FIJI plugins. Differences in qAF8, stratified by lens status, PCO severity, and AMD status, were analyzed using generalized estimating equations.

Results: In 210 eyes of 115 individuals (mean age = 75.7 ± 6.6 years), qAF8 was lower in intermediate AMD compared to early AMD ($P = 0.05$). qAF8 did not differ between phakic and pseudophakic eyes ($P = 0.8909$). In phakic ($n = 83$) and pseudophakic ($n = 127$) eyes considered separately, qAF8 did not differ by AMD status ($P = 0.0936$ and 0.3494 , respectively). Qualitative review of qAF images in phakic eyes illustrated high variability. In pseudophakic eyes, qAF8 did not differ with PCO present versus absent (54.5% vs. 45.5%). Review of implanted intraocular lenses (IOLs) revealed that 43.9% were blue-filter IOLs.

Conclusions: qAF8 was not associated with AMD status, up to intermediate AMD, considering only pseudophakic eyes to avoid noisy images in phakic eyes. In pseudophakic eyes, qAF8 was not affected by PCO. Because blue-filter IOLs may reduce levels of exciting light for qAF8, future studies investigating qAF in eyes with different IOL types are needed.

Translational Relevance: To reduce variability in observational studies and clinical trials requiring qAF8, pseudophakic participants without blue-filter IOLs or advanced PCO should be preferentially enrolled.

Introduction

Age-related macular degeneration (AMD) degrades sight in older adults worldwide,^{1,2} and involves dysfunction of the retinal pigment epithelium (RPE).³ To prevent vision loss, further understanding of RPE

health at different AMD stages is sought. A valuable tool for clinically visualizing RPE homeostasis and metabolism is fundus autofluorescence (FAF) imaging, a projection image of all chorioretinal layers.⁴

Quantitative fundus autofluorescence (qAF) uses an internal reference to normalize FAF intensity⁵ and enables comparison of eyes between study groups and

over time within individual patients.^{6–8} Currently used primarily in studies of inherited retinopathies, qAF has revealed disease activity in photoreceptors and RPE associated with specific gene mutations.^{9–13} Recent qAF studies of early and intermediate AMD eyes have shown a signal similar to or less than that in healthy controls.^{14,15}

The principal subcellular signal source of blue FAF (excitation wavelength, 488 nm) is RPE lipofuscin and melanolipofuscin.^{16–19} These organelles derived from photoreceptor outer segment tips accumulate in RPE cell bodies starting in childhood,²⁰ in a topography precisely linked to the photoreceptors.^{18,21–23} Bis-retinoid derivatives of vitamin A are suspected as the fluorophores underlying human FAF.²⁴ Increased and decreased FAF signal in AMD are impacted by RPE morphology and organelle content as well as adjacent tissue layers that add to or block the signal.^{16,25,26} Expansion of an area of a markedly reduced FAF signal is approved as a clinical trial end point, representing late stage disease.^{27,28} The idea that an FAF signal might increase in earlier AMD stages was initially supported by model systems and low-spatial resolution human eye pathology (e.g. assays of whole eyecups).²¹ Recent studies showing lipofuscin redistribution and loss as well as stacking and migration of RPE cells in AMD well before atrophy suggests that a decreased or variable signal is likely.²⁶

The optical density and autofluorescence of the crystalline lens increase with age and vary from person to person, impacting all fundus imaging and especially blue FAF/qAF imaging.^{29–33} The aged lens absorbs ultraviolet light and limits its transmission to and from the retina.⁵ How the aged lens influences qAF imaging is currently only partly understood.³⁴ To correct the qAF signal for lens opacity, a universal correction factor for age has been established.^{5,6,29} However, a single factor may not adequately compensate for wide individual differences of lens opacification.

In industrialized countries, age-related lens opacity is routinely addressed by cataract extraction and surgical implantation of intraocular lenses (IOLs).^{35–38} Because half of Americans older than 75 years have IOLs,³⁹ it is useful to know if the IOL itself or follow-on procedures affect qAF imaging. IOLs have a range of light transmission properties, and some selectively reduce blue light in addition to ultraviolet light. Further, a complication of cataract surgery, called posterior capsule opacification (PCO), reduces central light transmission and visual acuity in about 28% of eyes after 5 years (Fig. 1).⁴⁰ Fibrotic PCO represents connective tissue transformation of the lens capsule, whereas regenerative PCO represents proliferation of

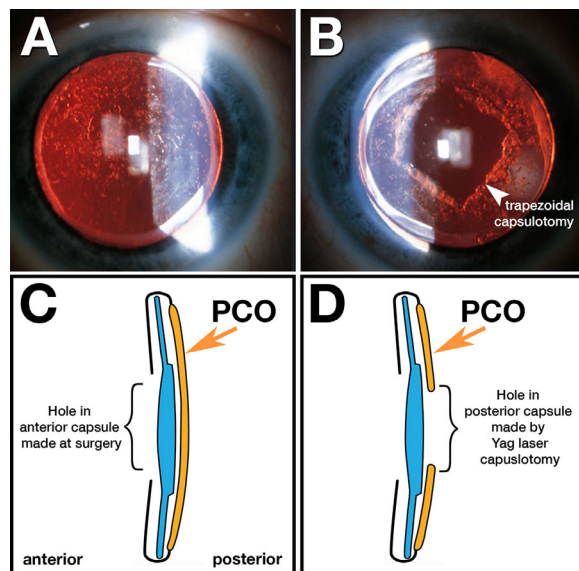


Figure 1. Posterior capsular opacification following intraocular lens implant. Posterior capsular opacification (PCO) is corrected with a capsulotomy, performed with a neodymium-doped yttrium aluminum garnet (Nd:YAG) laser. (A, B) Reflected light in retroillumination of the same eye, pre- and post-laser treatment (for illustration purpose only; this eye was not included in the study. This capsulotomy is less than 6 mm diameter. Thereby the remaining opacity might impact the quality of qAF images). (C, D) Schematics show a lateral view. A and C Severe PCO (grade 4) in a pseudophakic 2 years after surgery and before laser capsulotomy. B and D PCO after laser capsulotomy. B The opened PCO is thick at the trapezoidal capsulorhexis margin. D The posterior capsule is opened, and some PCO remains. De-identified clinical images courtesy of Arno Sailer, MD, Kolsass, Austria.

epithelial cells remaining on the capsule surface.⁴¹ To restore light transmission and acuity, a neodymium:yttrium-aluminum-garnet (Nd:YAG) capsulotomy is currently the gold standard.⁴¹

Our purpose herein was to investigate perifoveal qAF at 6 degrees to 8 degrees eccentricity (qAF8) in patients with and without early or intermediate AMD. We compared qAF8 in phakic and pseudophakic eyes, and, among pseudophakic eyes, we investigated the impact of PCO.

Methods

Compliance

This study was approved by the institutional review board at the University of Alabama at Birmingham (protocol # 170324006). It adhered to the tenets of the Declaration of Helsinki and complied with the Health Insurance Portability and Accountability Act of 1996.

Study Population

Participants were recruited from comprehensive ophthalmic practices in the Callahan Eye Hospital Clinics during 2017 to 2018, as described.^{42,43} To be eligible, eyes were required to meet fundus criteria for normal macular health, early AMD, or intermediate AMD. For comparison with existing qAF literature in AMD, eyes were graded using three-field digital stereo color fundus photographs (Carl Zeiss Meditec 450+, Dublin, CA) by an experienced and masked grader (author M.E.C.) using the Beckman classification system.⁴⁴ Previous diagnoses of glaucoma, other retinal conditions, optic nerve conditions, corneal disease, diabetes, Alzheimer's disease, Parkinson's disease, brain injury, and other neurological or psychiatric conditions as revealed by the medical record or by self-report were exclusion criteria.

Demographic characteristics (age, sex, and race/ethnicity) were obtained via participant interview. Lens status was determined by the anterior segment slit lamp photographs (Carl Zeiss Meditec 450+). For IOLs in pseudophakic participants, the manufacturer and model were determined from the medical record. PCO status was determined by slit lamp assessment, as indicated in the clinic electronic health record. PCO status was categorized as "present" and "not present." "Not present" included either a clear posterior capsule or an open posterior capsule after laser capsulotomy. PCO severity was classified as trace, 1+, 2+, and 3+ in the clinical record, following published grading systems.⁴⁵ Eyes lacking record of PCO status were excluded from the PCO analysis. Ophthalmologic assessments included measurement of corneal curvatures (IOL Master; Carl Zeiss) and best corrected visual acuity using the Electronic Visual Acuity tester (EVA; JAEB Center, Tampa, FL) under photopic conditions (100 cd/m²) and expressed as the logarithm of the minimum angle of resolution (logMAR).

Clinical Image Capture and Analysis

For multimodal imaging, eyes were dilated to a minimum of 6.5 mm pupil diameter using 0.5% tropicamide and 2.5% phenylephrine. Multimodal imaging included qAF, near infrared reflectance (NIR), and spectral-domain optical coherence tomography (OCT; 6-mm horizontal macular scan, 35 frames, 49 B-scans, 20 degrees × 20 degrees field) using a Spectralis device (Heidelberg Engineering, Heidelberg, Germany) modified for qAF as described.⁸ All images were adjusted using participant corneal c-curves for calculation of an individual scaling factor.⁶

Briefly, the Spectralis device contains an internal qAF reference that is excited simultaneously with the fundus (image size = 30 × 30, 768 × 768 pixels, excitation 488 nm and emission = 500–750 nm). In this way, variations in laser power and camera settings between examinations or between subjects can be normalized. To reduce FAF signal attenuation by rod photopigment, photoreceptors were bleached for at least 20 seconds before registration of 12 single FAF gray scale measurement frames.^{5,46} These frames were immediately checked for homogeneous illumination of the posterior pole and centration of the image on the fovea. Low-quality frames were removed from consideration at this time. The remaining image frames were used to create an average gray scale FAF image using the manufacturer's software. Subjects were excluded from further analysis if fewer than nine frames were useable.

qAF was described by Delori et al.⁵ to analyze gray scale measurements in an averaged AF image. Kleefeldt et al.⁸ extended this approach using custom plugins for FIJI (FIJI Is Just; ImageJ 2.0.0-rc-69/1.52p; www.fiji.sc; available at: <https://sites.imagej.net/CreativeComputation/>). qAF in an individual eye represents mean gray value of each pixel relative to that measured through the optical media of an emmetropic eye of a 20-year-old.^{5,6} The qAF correction for media (cornea, aqueous, lens, and vitreous), in turn, incorporated templates for light absorption based on extensive literature review by van de Kraats and van Norren.²⁹

To compare qAF between and within subjects we used qAF8,^{5,6} defined as mean pixel intensities in a ring of 8 evenly spaced segments, in the perifovea, at 6 degrees to 8 degrees eccentricity. A previous description of 9 degrees to 11 degrees for this location was incorrect.⁸ qAF8 was chosen by its originators to avoid blocking of the signal by macular pigment and to reduce signal noise due to non-autofluorescent vessels at the arcades.^{5,6} Placement of the qAF8 ring in most prior literature was based on the examiner's visual impression of the position of the fovea and the optic disc. Thus, to standardize anatomic landmarks in a Cartesian coordinate system, we used the "Find Fovea OCT" plugin⁸ on the macular OCT volume and corresponding NIR image, as described.⁸ Within the OCT B-scan, the position of the fovea was selected at the maximal rise of the external limiting membrane (central bouquet)^{47–49} within the foveal pit. Next, the edge of the optic nerve head closest to the fovea was marked.

We then used the "QAF XML Reader" plugin⁸ to enter the subject's age to compensate for attenuation of qAF signal by age-related media changes.^{5,6,29} At this time, a device-specific calibration factor (provided

by Heidelberg Engineering) was also entered.^{5,6} For phakic eyes, the participant's age was entered for a "one-size-fits-all" correction. For pseudophakic eyes, no correction was made, per convention.^{5,6} qAF images were registered to the NIR image using the "Register OCT" plugin.⁸ qAF was then derived using the "Batch Grids OCT" plugin⁸ and stored in tab-delimited text files for calculation of qAF8 and statistical analysis. Color-coded maps generated from gray scale images were used for qualitative analysis.

Statistical Analysis

Demographic, best-corrected visual acuity, AMD status and severity, and PCO status were summarized using means and standard deviations or number and percent for continuous and categorical data, respectively. Generalized estimating equations, which account for 2 eyes, were used to compare qAF8 by lens status, AMD status and severity, and PCO status and severity. In addition, each AMD severity category was compared to each other in pairwise comparisons. All models were age adjusted and the level of significance was $P \leq 0.05$ (2-sided). All analyses were done in SAS version 9.4.

Results

Of 230 examined eyes, 20 were excluded from analysis due to poor image quality, leaving 210 eyes from 115 individuals (mean age = 75.7 ± 6.6 years, 47 women [40.9%]). Demographic information for participants is summarized in Table 1. Eye-level data are shown in Table 2. These include AMD presence and severity ($n = 79$ [37.6%] normal, 53 [25.2%] early AMD, and 78 [37.1%] intermediate AMD), and lens status (83 phakic and 127 pseudophakic eyes). Phakic and pseudophakic eyes had similar proportions of normal, early AMD,

Table 1. Demographic Characteristics of Participants ($N = 115$)

Characteristic	Value
Age, y, mean (SD)	75.7 (6.6)
Age group, n (%)	
60–69	19 (16.5)
70–79	69 (60.0)
80–89	23 (20.0)
90–100	4 (3.5)
Gender, n (%)	
Male	68 (59.1)
Female	47 (40.9)
Race, n (%)	
White	111 (96.5)
African American	3 (2.6)
Asian or Pacific Islander	1 (0.9)

and intermediate AMD eyes (37.4%, 15.7%, and 47.0% vs. 30.7%, 22.8%, and 46.5%, respectively). Among all eyes, the average participant age was 75.3 ± 4.7 , 74.0 ± 6.2 , and 76.0 ± 7.6 years for those judged with normal, early, and intermediate AMD, respectively. Participants with pseudophakic eyes were older, 77.3 ± 5.9 years, relative to phakic eyes (72.3 ± 6.3). Characteristics of implanted IOLs are displayed in Supplementary Table S1. Information was retrievable for 66 (51%) of 127 pseudophakic eyes. Implanted IOL were mainly monofocal (84.8%) with a few toric (15.2%). Blue light filter IOLs (400–475 nm) were implanted in 29 (43.9%) of 66 eyes.

We first consider the impact of AMD status. Differences in qAF8 among disease severity groups were significant, when the entire sample of eyes was considered ($P = 0.05$; Table 3). Mean qAF8 was higher by 5.2% in early AMD eyes than normal eyes and lower by 18.7% in intermediate AMD eyes than in early AMD eyes. Pairwise comparison of qAF8 by disease status in the entire sample of phakic and pseudophakic

Table 2. AMD Status (Beckman Classification System) and Best Corrected Visual Acuity

Characteristic	All Eyes (N Eyes = 210)	Phakic Eyes (N Eyes = 83)	Pseudophakic Eyes (N Eyes = 127)
AMD status, n (%)			
Normal	79 (37.6)	31 (37.4)	39 (30.7)
Early	53 (25.2)	13 (15.7)	29 (22.8)
Intermediate	78 (37.1)	39 (47.0)	59 (46.5)
Visual function			
Best-corrected visual acuity (logMAR), mean (std)	0.09 (0.19)	0.07 (0.13)	0.10 (0.21)

Std, standard deviation.

Table 3. Comparison of qAF₈ Values by AMD Status and Severity Classified Using the Beckman Scales Judged Normal, Early, or Intermediate AMD

Disease status	n (%) of Eyes	Mean (std) ^c	P Value ^b
A. All eyes (N persons = 115, N eyes = 210)^a			
			0.0500
Normal	70 (33.3)	228.4 (77.2)	
Early	42 (20.0)	240.1 (71.2)	
Intermediate	98 (46.7)	(71.8)	
B. Phakic eyes (N persons = 47, N eyes = 83)			
			0.0936
Normal	31 (37.4)	241.2 (80.9)	
Early	13 (15.7)	249.3 (49.9)	
Intermediate	39 (47.0)	(81.0)	
C. Pseudophakic eyes (N persons = 74, N eyes = 127)			
			0.3494
Normal	39 (30.7)	218.3 (73.6)	
Early	29 (22.8)	236.0 (79.4)	
Intermediate	59 (46.5)	191.5 (65.4)	

^aPairwise comparison of qAF₈ by disease status in all eyes: normal versus early AMD $P = 0.2038$; normal versus intermediate AMD $P = 0.3678$; early versus intermediate AMD $P = 0.0152$.

^bComparison by AMD status and severity from generalized estimating equations adjusting for age.

^cBetween phakic and pseudophakic eyes there was no significant difference in qAF₈ variability, as assessed by the mean minimum, maximum, and standard deviation of the collected data (P values 0.3989, 0.1864, and 0.6385, respectively).

Std, standard deviation.

eyes showed a significant difference only between early and intermediate AMD ($P = 0.0152$). The pairwise comparisons of normal versus early AMD and normal vs intermediate AMD, in the entire sample of phakic and pseudophakic eyes, were not significant ($P = 0.2038$ and $P = 0.3678$, respectively). Considering either phakic or pseudophakic eyes separately, the qAF₈ values did not differ significantly among normal, early, or intermediate AMD in either group (see Table 3).

Table 4. Quantitative Fundus Autofluorescence in all Eyes, Stratified by Lens Status

	All Eyes (N Eyes = 210)	Phakic Eyes (N Eyes = 83)	Pseudophakic Eyes (N Eyes = 127)	P Value ^a
qAF ₈ , mean (std)	215.3 (75.7)	223.7 (79.1)	209.9 (73.1)	0.8909

^aComparison between phakic and pseudophakic eyes from generalized estimating equations adjusting for age. Std, standard deviation.

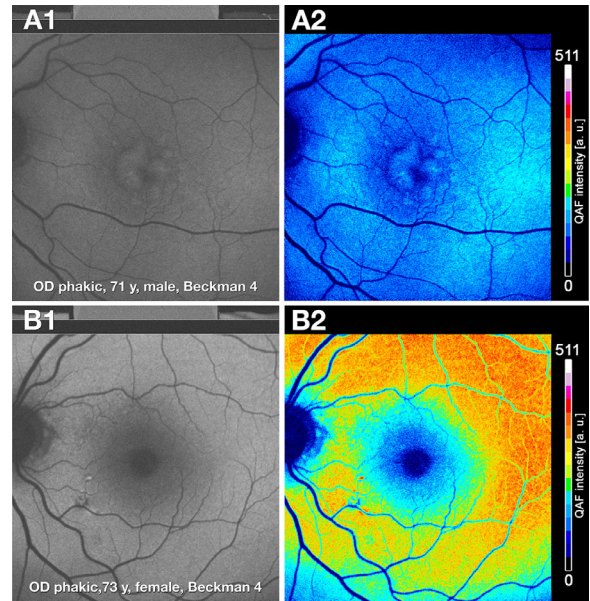


Figure 2. Impact of crystalline lens on autofluorescence appearance and qAF. (A1, A2) In an aged phakic eye, qAF images are blurred and dim in grayscale and low intensity in color-coded images (A2). (B1, B2) A comparison eye of similar age and early AMD status shows a less blurred and brighter gray scale qAF image, compared to A1. The color-coded qAF image B2 contains higher and more distinct qAF intensity levels than A2. Lens color and opacification grading not available.

The impact of natural and implanted IOLs on qAF₈ is considered next. Comparing phakic and pseudophakic eyes, no overall difference in qAF₈ was detected (mean \pm standard deviation: phakic = 223.7 ± 79.1 and pseudophakic = 209.9 ± 73.1 , $P = 0.8909$; Table 4). Among pseudophakic eyes, the qAF₈ did not differ significantly by PCO status and severity (Table 5), although only 10% of pseudophakic eyes had moderate or advanced PCO (+2 and +3).

To elucidate why qAF₈ was related to AMD only when phakic and pseudophakic eyes are combined, we next illustrate examples of qAF variability introduced by the aging lens. Figure 2 shows phakic eyes of similar chronologic age. Gray scale images (Figs. 2A1, 2B1) differed in brightness, image focus, and contrast, depending on crystalline lens characteristics. Color-coded qAF values when correctly adjusted for age showed markedly higher qAF intensity in superior and

Table 5. qAF₈ Stratified by PCO Presence and Severity (N Persons = 57, N eyes = 99)

PCO Categorization	n (%) of Eyes	Mean qAF8 (std)	P Value ^a
PCO status and severity			0.3296
Clear	22 (22.2)	217.9 (68.3)	
Trace	8 (8.1)	205.4 (64.6)	
1+	14 (14.1)	202.4 (61.8)	
2+ or 3+	10 (10.1)	196.5 (63.0)	
Open (after laser capsulotomy)	45 (45.5)	214.7 (72.1)	
PCO yes/no, "clear" or "open"			0.1296
Open or clear	67 (67.7)	215.8 (70.4)	
Trace to 3+	32 (32.3)	201.3 (75.2)	

^aComparison by PCO status and severity category from generalized estimating equations. Std, standard deviation.

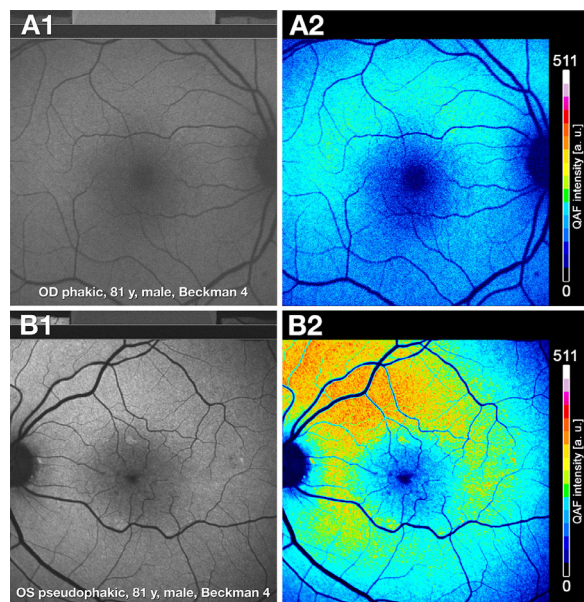


Figure 3. Quantitative autofluorescence in phakic and pseudophakic fellow eyes. (A1, A2) In an aged phakic eye, qAF grayscale image is blurred and dim, and the color coded qAF image has low intensity A2. Lens color and opacification grading not available. (B1, B2) In a pseudophakic qAF grayscale image with clear view and high level of detail of the posterior pole in the pseudophakic fellow eye of the same patient as in A. The corresponding color coded qAF image B2 contains higher and more distinct levels of qAF intensity. Both images displayed markedly increased qAF intensity in the superior perifovea.

superior-perifoveal regions (Figs. 2A2, 2B2). Figure 3 shows a striking difference between a phakic and pseudophakic eye, at the same AMD severity level, in one participant. In the phakic eye, the qAF gray scale image is blurred and dim (see Fig. 3A1), and the color coded qAF image has low intensity (see Fig. 3A2). In the pseudophakic eye, the qAF grayscale image provides a clear fundus view and displays a high level of

detail (see Fig. 3B1). Further, the corresponding color coded qAF image contains higher and more distinct levels of qAF intensity (see Fig. 3B2).

Discussion

For maximal clinical utility, qAF must address individual variation in the lifespan accumulation of retinal FAF,^{6,8,50} lens opacity, and autofluorescence in older persons with crystalline lenses. In pseudophakic eyes, it is possible that the implanted IOL itself, depending on spectral characteristics, or post-surgery PCO will impact light transmission. Our main finding is that qAF₈ is lower in intermediate AMD than in early AMD, if phakic and pseudophakic eyes are combined, and not if they are analyzed separately.

Although decreased qAF₈ in intermediate AMD comports with our expectations from histology, we currently interpret these results cautiously. First, this decrease was driven by changes in phakic eyes, not pseudophakic eyes. Figures 2 and 3 amply demonstrate the inherent variability introduced by the aging lens. Second, in these phakic eyes, the highest qAF₈ occurred in early AMD. In the Beckman grading system, this stage does not include pigmentary changes that might lead to increased signal by rounding or stacking of RPE. Previous qAF studies assessing comparable stages of AMD, also using the Beckman scale^{51–54} (Table 6), similarly concluded that qAF in early and intermediate AMD does not differ significantly from healthy controls.^{14–15} Owing to differences in study design, the similar outcomes may be fortuitous. Several reasons may underlie modest or minimal differences between controls and intermediate AMD collectively revealed by qAF₈ in the current study and those in Table 6. First, as decreased qAF

Table 6. qAF Studies in Early and Intermediate AMD

Author	Demographics (Eyes/Patients)	Lens Status	AMD Groups	Results
Gliem 2016 ^{14a}	<i>n</i> = 40/40 age = 54.8 ± 5.6 y 108 controls	p	28 SD; 8 CD 4 eAMD; 36 iAMD	no significant qAF8 difference in eAMD-iAMD versus control
Orellana-Rios 2018 ⁵³	<i>n</i> = 31/31 age = 83.9 ± 5.39 y 36 controls	pp	17 SD/CD 11 RMD/SDD 8 GA	Mean qAF8 higher in controls than in AMD patients (<i>P</i> < 0.001) Significant qAF8 difference SDD versus controls (<i>P</i> < 0.05) Lowest mean qAF8 in GA
Reiter 2019 ^{52b}	<i>n</i> = 88/52 age = 75.6 ± 5.0 y 0 controls	46 (52%) cat ^c 42 (48%) pp	eAMD, iAMD	No significant association of qAF and drusen volume qAF decreases with age in AMD (<i>P</i> = 0.025); drusen volume increases with age
Reiter 2020 ⁵¹	<i>n</i> = 43/22 age = 73.5 ± 7.9 y 0 controls	24 (56%) cat ^c 19 (44%) pp	eAMD, iAMD	Excellent repeatability, reliability, follow-up agreement in eAMD and iAMD
Reiter 2021 ⁵⁴	<i>n</i> = 121/71 age = 74.4 ± 5.5 y 0 controls	71 (59%) cat ^c 50 (41%) pp	121 eyes with iAMD; 21 converted to late AMD	Declining qAF associated with developing atrophic AMD (<i>P</i> < 0.001)
Von der Emde 2021 ¹⁵	<i>n</i> = 85/51 age = 71 ± 7 y 51 controls	68 (80%) p 17 (20%) pp	iAMD	No significant qAF8 difference between AMD eyes with large drusen and healthy eyes (<i>P</i> = 0.130) Lower qAF8: pp (<i>P</i> = 0.010), male (<i>P</i> = 0.008) image quality (<i>P</i> = 0.001)
Berlin 2021 (current)	<i>n</i> = 210/115 age = 75.7 ± 6.6 y 79 controls	83 (40%) p 127 (60%) pp	53 eAMD, 78 iAMD	No significant difference in qAF8 in p versus pp eyes; PCO presence and severity; normal versus eAMD and iAMD.

cat, cataract; CD, cuticular drusen; eAMD, early AMD; GA, geographic atrophy; iAMD, intermediate AMD; o-c, observational, cross-sectional; o-l, observational longitudinal; p, phakic; PCO, posterior capsular opacification; pp, pseudophakic; SD, soft drusen; RMD, reticular macular disease; SDD, subretinal drusenoid deposits.

All studies used the Beckman Classification System; none of these studies mentioned PCO status

^aqAF parameter: horizontal band through the fovea (gray scale histograms along a 3-pixel-wide band).

^bqAF parameter: qAFIM (inner and middle ring of Delori grid).

^cCataracts were graded as Lens Opacities Classification System III nuclear ≤3.0 or subcapsular ≤2.0 to be included in the data.

presages geographic atrophy/complete RPE and outer retinal atrophy (cRORA),^{54–57} our study eyes may have been positioned too early in AMD progression to register marked qAF8 changes. Second, our model of AMD pathophysiology is deposit-driven end-stages of neovascularization and atrophy, wherein two layers of extracellular deposits (soft drusen and subretinal

drusenoid deposit) represent dysregulation of constitutive lipid transfer pathways specialized for cone and rod photoreceptors, respectively.^{58,59} In this scenario, the location of the qAF8 metric at 6 to 8 degrees eccentricity is not designed to probe the effect of high-risk AMD drusen in the central subfield and inner ring of the ETDRS grid (≤5.2 degrees eccentricity).

qAF8 is also not designed to probe areas near the arcades where rod density and AF signal are high and subretinal drusenoid deposits first appear.^{21,22,60} Third, qAF may not capture the most relevant predictors of visual decline in AMD. In a recent analysis of spectral domain OCT volumes, retinal locations that were highly predictive of performance on dark adaptation did not involve the RPE cell bodies (containing lipofuscin) but rather, sites on either side of the ellipsoid zone and the RPE-basal lamina-Bruch's membrane band.⁶¹ The latter may implicate changes in uptake and transfer functions of RPE apical processes and basal infoldings.

Prior studies (see Table 6) vary as to whether lens opacity and yellowing was assessed.^{14,15,51–54} Age-related lens yellowing from the modification of kynurenine compounds is also responsible for lens autofluorescence.^{62,63} As the lens opacifies, autofluorescence may be less apparent. Comparison of the same patient pre- and post-cataract surgery has helped define the impact of lens optical properties on imaging.^{34,64} Reiter et al. demonstrated that reconstituted qAF8 signals after cataract surgery were significantly associated with pre-operative cortical opacity grades.^{34,65} Although these authors concluded that age-related lens opacities must be incorporated into the interpretation of qAF8, they did not recommend a specific correction.³⁴

The literature reveals different ways that investigators mitigated the effect of lens aging in FAF-based retinal imaging. First, restricting study participant age to less than 60 years substantially avoids age-related lens opacification.⁵ A second approach is to objectively grade the extent of age-related changes and set a threshold for data exclusion.^{15,56,65} Third, it is possible to use excitation wavelengths longer than 488 nm to bypass short wavelength absorbers in the lens, an approach requiring a separate instrument in most cases.⁶⁶ Longitudinal data on individual eyes can potentially obviate some of the lens effects, because each patient serves as his or her own control over the observation period. For example, Von der Emde et al. reported a lack of significant differences in qAF8 between eyes with and without AMD and declining qAF over time only in the eyes with AMD.¹⁵ Reiter et al. found declining qAF over time, especially in eyes that converted to atrophic AMD.⁵⁴ We should recall that both lens and RPE may be changing at different rates over the same period. Clearly, a reliable means to correct for lens opacity and autofluorescence on an individual basis would be an important step forward for retinal FAF imaging.

We were surprised to learn that 43% of IOLs in pseudophakic patients in our study were of the type

that selectively reduce transmission of blue light. The number of eyes for which lens type could be determined was small, and some surgeries were done years prior to qAF imaging. Prior qAF imaging studies (see Table 6) did not mention blue-filter IOLs among pseudophakic eyes in their samples. Eyes with blue-blocking IOLs may impact qAF imaging by reducing a small proportion of light at the excitation wavelength of 488 nm.⁶⁷ Determining how much reduction is of importance, but it was beyond the scope of this study, which was retrospective with regard to the IOL inquiry. Prior studies (see Table 6) also did not consider the effect of PCO in pseudophakic eyes on qAF imaging.^{14,15,51–54} Our data thus add novelty to existing literature by suggesting that mild or moderate PCO status does not affect qAF values.

Strengths of our study are qAF8 values from the largest number of normal aged eyes ($n = 70$) and pseudophakic eyes ($n = 127$) to date, novel findings on PCO, and perspective from recent clinical and laboratory findings in human eyes. Limitations include a relatively small sample, and a very small number of eyes with advanced PCO. Further, PCO status was obtained retrospectively via electronic health record review, and no information about the capsulotomy technique and size was available. Age changes of the crystalline lens were not objectively graded. IOL characteristics were available for only half of the pseudophakic eyes, and these were heterogeneous with respect to optic type and transmission spectrum.

Despite these limitations, our analysis suggests that qAF8 is minimally affected up to intermediate AMD, changes in phakic eyes are due to lenticular effects, and qAF8 in pseudophakic eyes is not affected by the presence of moderate PCO. To maximize the clinical utility of qAF, future studies investigating qAF in eyes with different IOL types are needed. In the meantime, we recommend that studies assessing qAF8 in aged patients enroll only pseudophakic eyes without blue-filter IOLs and advanced PCO, to reduce variability. The lack of significant qAF8 differences along the progression from normal to early and intermediate AMD should be confirmed in a larger sample, such as our ongoing prospective observational study.

We draw five broader conclusions from these data. First, fundus AF remains an excellent imaging technology for assessing outer retinal integrity and health in early stages of AMD. Second, qAF offers advantages for comparative studies that can be improved by correction for lenses on an individual basis. Third, qAF8 is a less-than-ideal metric for AMD, because it does not assess sites of key pathology. Fourth, qAF measured at selected locations, at a spatial scale comparable to histology,^{8,17,68,69} and in reference to

a normative database,⁸ has potential that should be explored further. Finally, as reviewed,⁷⁰ the value of blue-blocking IOLs for preventing AMD is questionable, and they permanently reduce useful spectrum for rod-mediated vision.^{71,72} Whether they also impact the utility of FAF imaging for early stages of AMD needs further research.

Acknowledgments

Supported by R01EY029595 (to C.O. and C.A.C.) and R01EY027948 (to C.A.C.); P30EY03039 (to C.O.); Dorsett Davis Discovery Fund, and Alfreda J. Schueler Trust (to C.O.); Dr. Werner Jackstädt-Foundation (to A.B.); and unrestricted funds to the Department of Ophthalmology and Visual Sciences (UAB) from Research to Prevent Blindness, Inc., and EyeSight Foundation of Alabama.

Financial disclosure: C.A.C. receives research funds from Genentech/Hoffman LaRoche and Regeneron and consults for Apellis (outside this project).

Disclosure: **A. Berlin**, (N); **M.E. Clark**, (N); **T.A. Swain**, (N); **N.A. Fischer**, (N); **G. McGwin**, (N); **K.R. Sloan**, (N); **C. Owsley**, (N); **C.A. Curcio**, (C, F)

References

1. Flaxman SR, Bourne RR, Resnikoff S, et al. Global causes of blindness and distance vision impairment 1990–2020: a systematic review and meta-analysis. *The Lancet Global Health*. 2017;5(12):e1221–e1234.
2. Schmitz-Valckenberg S, Pfau M, Fleckenstein M, et al. Fundus autofluorescence imaging. *Prog Retin Eye Res*. 2021;81:100893.
3. Fleckenstein M, Keenan TD, Guymer RH, et al. Age-related macular degeneration. *Nat Rev Dis Primers*. 2021;7(1):1–25.
4. Yung M, Klufas MA, Sarraf D. Clinical applications of fundus autofluorescence in retinal disease. *Intl J Retina Vitreous*. 2016;2(1):1–25.
5. Delori F, Greenberg JP, Woods RL, et al. Quantitative measurements of autofluorescence with the scanning laser ophthalmoscope. *Invest Ophthalmol Vis Sci*. 2011;52(13):9379–9390.
6. Greenberg JP, Duncker T, Woods RL, Smith RT, Sparrow JR, Delori FC. Quantitative fundus autofluorescence in healthy eyes. *Invest Ophthalmol Vis Sci*. 2013;54(8):5684–5693.
7. Armenti ST, Greenberg JP, Smith RT. Quantitative fundus autofluorescence for the evaluation of retinal diseases. *JoVE (Journal of Visualized Experiments)*. 2016(109):e53577.
8. Kleefeldt N, Bermond K, Tarau I-S, et al. Quantitative fundus autofluorescence: advanced analysis tools. *Trans Vis Sci Technol*. 2020;9(8):2.
9. Burke TR, Duncker T, Woods RL, et al. Quantitative Fundus Autofluorescence in Recessive Stargardt Disease. *Invest Ophthalmol Vis Sci*. 2014;55(5):2841–2852.
10. Sparrow JR, Duncker T, Woods R, Delori FC. Quantitative fundus autofluorescence in best vitelliform macular dystrophy: RPE lipofuscin is not increased in non-lesion areas of retina. *Adv Exp Med Biol*. 2016;854:285–290.
11. Gliem M, Müller PL, Birtel J, et al. Quantitative Fundus Autofluorescence in Pseudoxanthoma Elasticum. *Invest Ophthalmol Vis Sci*. 2017;58(14):6159–6165.
12. Duncker T, Tsang SH, Lee W, et al. Quantitative Fundus Autofluorescence Distinguishes ABCA4-Associated and Non-ABCA4-Associated Bull's-Eye Maculopathy. *Ophthalmology*. 2015;122(2):345–355.
13. Gliem M, Müller PL, Birtel J, et al. Quantitative fundus autofluorescence and genetic associations in macular, cone, and cone-rod dystrophies. *Ophthalmol Retina*. 2020;4(7):737–749.
14. Gliem M, Müller PL, Finger RP, McGuinness MB, Holz FG, Issa PC. Quantitative fundus autofluorescence in early and intermediate age-related macular degeneration. *JAMA Ophthalmol*. 2016;134(7):817–824.
15. von der Emde L, Guymer RH, Pfau M, et al. Natural History of Quantitative Autofluorescence in Intermediate Age-Related Macular Degeneration. *Retina*. 2021;41(4):694–700.
16. Gambriel JA, Sloan KR, Swain TA, et al. Quantifying retinal pigment epithelium dysmorphia and loss of histologic autofluorescence in age-related macular degeneration. *Invest Ophthalmol Vis Sci*. 2019;60(7):2481–2493.
17. Bermond K, Berlin A, Tarau I-S, et al. Characteristics of normal human retinal pigment epithelium cells with extremes of autofluorescence or intracellular granule count. *Ann Eye Sci*. 2021; 6:3.
18. Bermond K, Wobbe C, Tarau I-S, et al. Autofluorescent granules of the human retinal pigment epithelium: phenotypes, intracellular distribution, and age-related topography. *Invest Ophthalmol Vis Sci*. 2020;61(5):35.

19. Pollreisz A, Neschi M, Sloan KR, et al. Atlas of human retinal pigment epithelium organelles significant for clinical imaging. *Invest Ophthalmol Vis Sci.* 2020;61(8):13.
20. Feeney L. Lipofuscin and melanin of human retinal pigment epithelium. Fluorescence, enzyme cytochemical, and ultrastructural studies. *Invest Ophthalmol Vis Sci.* 1978;17(7):583–600.
21. Ach T, Huisinck C, McGwin G, et al. Quantitative autofluorescence and cell density maps of the human retinal pigment epithelium. *Invest Ophthalmol Vis Sci.* 2014;55(8):4832–4841.
22. Curcio CA, Sloan KR, Kalina RE, Hendrickson AE. Human photoreceptor topography. *J Comparative Neurol.* 1990;292(4):497–523.
23. Wing GL, Blanchard GC, Weiter JJ. The topography and age relationship of lipofuscin concentration in the retinal pigment epithelium. *Invest Ophthalmol Vis Sci.* 1978;17(7):601–607.
24. Kim HJ, Sparrow JR. Bisretinoid phospholipid and vitamin A aldehyde: Shining a light. *J Lipid Res.* 2021;62:100042.
25. Chen L, Messinger JD, Ferrara D, Freund KB, Curcio CA. Fundus autofluorescence in neovascular age-related macular degeneration, a clinicopathologic correlation relevant to macular atrophy. *Ophthalmol Retina.* 2021;5(11):1085–1096.
26. Chen L, Messinger JD, Ferrara D, Freund KB, Curcio CA. Stages of drusen-associated atrophy in age-related macular degeneration visible via histologically validated fundus autofluorescence. *Ophthalmol Retina.* 2021;5(8):730–742.
27. Holz FG, Sadda SR, Staurenghi G, et al. Imaging protocols in clinical studies in advanced age-related macular degeneration: recommendations from classification of atrophy consensus meetings. *Ophthalmology.* 2017;124(4):464–478.
28. Csaky K, Ferris F, Chew EY, Nair P, Cheetham JK, Duncan JL. Report from the NEI/FDA endpoints workshop on age-related macular degeneration and inherited retinal diseases. *Invest Ophthalmol Vis Sci.* 2017;58(9):3456–3463.
29. Van De Kraats J, Van Norren D. Optical density of the aging human ocular media in the visible and the UV. *JOSA A.* 2007;24(7):1842–1857.
30. Satoh K, Bando M, Nakajima A. Fluorescence in human lens. *Exp Eye Res.* 1973;16(2):167–172.
31. Gakamsky A, Duncan RR, Howarth NM, et al. Tryptophan and non-tryptophan fluorescence of the eye lens proteins provides diagnostics of cataract at the molecular level. *Sci Rep.* 2017;7(1):1–15.
32. Occhipinti JR, Mosier MA, Burstein NL. Autofluorescence and light transmission in the aging crystalline lens. *Ophthalmologica.* 1986;192(4):203–209.
33. Charng J, Tan R, Luu CD, et al. Imaging lenticular autofluorescence in older subjects. *Invest Ophthalmol Vis Sci.* 2017;58(12):4940–4947.
34. Reiter GS, Schwarzenbacher L, Schartmüller D, et al. Influence of lens opacities and cataract severity on quantitative fundus autofluorescence as a secondary outcome of a randomized clinical trial. *Sci Rep.* 2021;11(1):1–9.
35. Owsley C, McGwin G, Jr, Searcey K. A population-based examination of the visual and ophthalmological characteristics of licensed drivers aged 70 and older. *J Gerontol A Biol Sci Med Sci.* 2013;68(5):567–573.
36. Ianchulev T, Litoff D, Ellinger D, Stiverson K, Packer M. Office-based cataract surgery: population health outcomes study of more than 21 000 cases in the United States. *Ophthalmology.* 2016;123(4):723–728.
37. Lundström M, Dickman M, Henry Y, et al. Changing practice patterns in European cataract surgery as reflected in the European Registry of Quality Outcomes for Cataract and Refractive Surgery 2008 to 2017. *J Cataract Refractive Surg.* 2021;47(3):373–378.
38. Eurostat. Surgical operations and procedures statistics. Available at: https://ec.europa.eu/eurostat/statistics-explained/index.php?title=Surgical_operations_and_procedures_statistics#Number_of_surgical_operations_and_procedures. Published September 2020. Updated September 2020. Accessed December 4, 2021.
39. The-Vision-Council. 2019 Vision Watch Cataract Report. Available at: <https://eyewire.news/articles/the-vision-council-releases-2019-vision-watch-ataract-report>. Published 2019. Accessed December 4, 2021.
40. Schaumberg DA, Dana MR, Christen WG, Glynn RJ. A systematic overview of the incidence of posterior capsule opacification. *Ophthalmology.* 1998;105(7):1213–1221.
41. Wormstone I, Wormstone Y, Smith A, Eldred J. Posterior capsule opacification: What's in the bag? *Prog Retinal Eye Res.* 2021;82:100905.
42. Kar D, Clark ME, Swain TA, et al. Local Abundance of Macular Xanthophyll Pigment Is Associated with Rod-and Cone-Mediated Vision in Aging and Age-Related Macular Degeneration. *Invest Ophthalmol Vis Sci.* 2020;61(8):46.
43. Echols BS, Clark ME, Swain TA, et al. Hyper-reflective foci and specks are associated with

- delayed rod-mediated dark adaptation in nonneovascular age-related macular degeneration. *Ophthalmology Retina*. 2020;4(11):1059–1068.
44. Ferris F., Wilkinson CP, Bird A, et al. Clinical classification of age-related macular degeneration. *Ophthalmology*. 2013;120:844–851.
 45. Aslam T, Dhillon B, Werghi N, Taguri A, Wadood A. Systems of analysis of posterior capsule opacification. *Br J Ophthalmol*. 2002;86(10):1181–1186.
 46. Theelen T. Scanning laser imaging of the retina. Basic concepts and clinical applications. Available at: https://www.researchgate.net/publication/232768942_Scanning_Laser_Imaging_of_the_Retina_-_Basic_Concepts_and_Clinical_Applications. 2011.
 47. Rochon-Duvigneaud A. Recherches sur la fovea de la rétine humaine et particulièrement sur le bouquet des cônes centraux. *Arch Anat Microsc*. 1907;9:315–342.
 48. Ahnelt P. The photoreceptor mosaic. *Eye*. 1998;12(3):531–540.
 49. Kolb H, Nelson RF, Ahnelt PK, Ortuño-Lizarán I, Cuenca N. The architecture of the human fovea. In: *Webvision: The Organization of the Retina and Visual System [Internet]*. Salt Lake City, UT: University of Utah Health Sciences Center; 1995. 2020. [updated May 20, 2020].
 50. Pröbster C, Tarau I-S, Berlin A, et al. Quantitative fundus autofluorescence in the developing and maturing healthy eye. *Transl Vis Sci Technol*. 2021;10(2):15.
 51. Reiter GS, Told R, Baratsits M, et al. Repeatability and reliability of quantitative fundus autofluorescence imaging in patients with early and intermediate age-related macular degeneration. *Acta Ophthalmologica*. 2019;97(4):e526–e532.
 52. Reiter GS, Told R, Schlanitz FG, et al. Impact of drusen volume on quantitative fundus autofluorescence in early and intermediate age-related macular degeneration. *Invest Ophthalmol Vis Sci*. 2019;60(6):1937–1942.
 53. Orellana-Rios J, Yokoyama S, Agee JM, et al. Quantitative fundus autofluorescence in non-neovascular age-related macular degeneration. *Ophthalmic Surg Lasers Imaging Retina*. 2018;49(10):S34–S42.
 54. Reiter GS, Hacker V, Told R, et al. Longitudinal changes in quantitative autofluorescence during progression from intermediate to late age-related macular degeneration. *Retina*. 2021;41(6):1236–1241.
 55. Holmen IC, Aul B, Pak JW, et al. Precursors and development of geographic atrophy with autofluorescence imaging: Age-related Eye Disease Study 2 report number 18. *Ophthalmol Retina*. 2019;3(9):724–733.
 56. Jaffe GJ, Chakravarthy U, Freund KB, et al. Imaging features associated with progression to geographic atrophy in age-related macular degeneration: classification of atrophy Meeting Report 5. *Ophthalmol Retina*. 2021;5(9):855–867.
 57. Domalpally A, Danis R, Agrón E, et al. Evaluation of geographic atrophy from color photographs and fundus autofluorescence images: Age-Related Eye Disease Study 2 report number 11. *Ophthalmology*. 2016;123(11):2401–2407.
 58. Spaide RF. Improving the age-related macular degeneration construct: a new classification system. *Retina*. 2018;38(5):891–899.
 59. Sadda SR, Schachat AP, Wilkinson CP, et al. *Ryan's Retina, Section 3, Pathogenesis of age-related macular degeneration*. New York, NY: Elsevier Health Sciences; 2022.
 60. Curcio CA. Photoreceptor topography in ageing and age-related maculopathy. *Eye*. 2001;15(3):376–383.
 61. Lee AY, Lee CS, Blazes MS, et al. Exploring a structural basis for delayed rod-mediated dark adaptation in age-related macular degeneration via deep learning. *Transl Vis Sci Technol*. 2020;9(2):62.
 62. Vazquez S, Aquilina JA, Jamie JF, Sheil MM, Truscott RJ. Novel protein modification by kynurenine in human lenses. *J Biol Chem*. 2002;277(7):4867–4873.
 63. Vazquez S, Parker NR, Sheil M, Truscott RJ. Protein-bound kynurenine decreases with the progression of age-related nuclear cataract. *Invest Ophthalmol Vis Sci*. 2004;45(3):879–883.
 64. Obana A, Gohto Y, Gellermann W, et al. Grade of cataract and its influence on measurement of macular pigment optical density by autofluorescence imaging. *Invest Ophthalmol Vis Sci*. 2018;59(9):4513–4513.
 65. Chylack LT, Wolfe JK, Singer DM, et al. The lens opacities classification system III. *Arch Ophthalmol*. 1993;111(6):831–836.
 66. Bird AC, Holz FG, Schmitz-Valckenberg S, Spaide RF. Autofluorescence imaging with the fundus camera. *Atlas of Fundus Autofluorescence Imaging*. New York, NY: Springer; 2007:49–54.
 67. Cuthbertson FM, Peirson SN, Wulff K, Foster RG, Downes SM. Blue light-filtering intraocular lenses: Review of potential benefits and side effects. *J Cataract Refractive Surg*. 2009;35(7):1281–1297.
 68. Ach T, Tolstik E, Messinger JD, Zarubina AV, Heintzmann R, Curcio CA. Lipofuscin

- redistribution and loss accompanied by cytoskeletal stress in retinal pigment epithelium of eyes with age-related macular degeneration. *Invest Ophthalmol Vis Sci.* 2015;56(5):3242–3252.
69. Rudolf M, Vogt SD, Curcio CA, et al. Histologic basis of variations in retinal pigment epithelium autofluorescence in eyes with geographic atrophy. *Ophthalmology.* 2013;120(4):821–828.
 70. Jackson G. Pilot study on the effect of a blue-light-blocking IOL on rod-mediated (scotopic) vision. *American Society for Cataract and Refractive Surgery: April.* 2005:15–20.
 71. Mainster MA, Turner PL. Blue-blocking IOLs decrease photoreception without providing significant photoprotection. *Survey of Ophthalmol.* 2010;55(3):272–283.
 72. Mainster MA, Findl O, Dick HB, et al. The Blue Light Hazard Versus Blue Light Hype. *Am J Ophthalmol.* 2022;240:51–57.